The Journal of Veterinary Medical Science

FULL PAPER

Anatomy

Effects of the expansion of bacterial colonies into the intervillous spaces on the localization of several lymphocyte lineages in the rat ileum

Hideto YUASA[1], Youhei MANTANI[2]*, Kazuki MIYAMOTO[2], Miho NISHIDA[2], Masaya ARAI[2], Hiroki TSURUTA[4], Toshifumi YOKOYAMA[3], Nobuhiko HOSHI[3] and Hiroshi KITAGAWA[2]

[1]Department of Anatomy and Regenerative Biology, Graduate School of Medicine, Osaka City University, 1-4-3 Asahi-machi, Abeno-ku, Osaka 545-8585, Japan
[2]Laboratory of Histophysiology, Department of Bioresource Science, Graduate School of Agricultural Science, Kobe University, 1-1 Rokkodai-cho, Nada-ku, Kobe, Hyogo 657-8501, Japan
[3]Laboratory of Molecular Morphology, Department of Bioresource Science, Graduate School of Agricultural Science, Kobe University, 1-1 Rokkodai-cho, Nada-ku, Kobe, Hyogo 657-8501, Japan
[4]Center for Collaborative Research and Technology Development, Kobe University, 1-1 Rokkodai-cho, Nada-ku, Kobe, Hyogo 657-8501, Japan

ABSTRACT. The effect of bacterial colonies expanded into the intervillous spaces on the localization of several lymphocyte lineages was immunohistochemically investigated in two types of mucosa: ordinary mucosa of rat ileum, which consists of mucosa without any mucosal lymphatic tissue; and follicle-associated mucosa (FAM), which accompanies the parafollicular area under the muscularis mucosae in the rat ileal Peyer's patch. The results showed that bacterial colonies in the intervillous spaces induced increased populations of $CD8^+$ cells in the epithelium of the intestinal villus in ordinary mucosa (IV) and intestinal villus in FAM (IV-FAM). Bacterial colonies in the intervillous spaces were also associated with increased numbers of IgA^+ cells, which were mainly localized in the lamina propria of basal portions of IV and IV-FAM, and with expanded localization of IgA^+ cells into the villous apex in both IV and IV-FAM. Moreover, IgA^+ cells around the intestinal crypts adjacent to IV or IV-FAM were also increased in response to bacterial colonies. In the IV-FAM, but not IV, L-selectin$^+$ cells, which were found to be immunopositive for TCRαβ or CD19, were drastically increased in the lamina propria from the crypt to middle portion of IV-FAM and in the lumen of central lymph vessel of IV-FAM in response to the bacterial colonies in the intervillous spaces. These findings revealed that the expansion of bacterial colonies into the intervillous spaces accompanies the change of histological localization of the lymphocyte lineage in both the ordinary mucosa and FAM.

KEY WORDS: ileum, immunohistochemistry, indigenous bacteria, lymphocyte, rat

J. Vet. Med. Sci.
81(4): 555–566, 2019
doi: 10.1292/jvms.18-0734

Received: 13 December 2018
Accepted: 13 February 2019
Published online in J-STAGE: 25 February 2019

Various types of immunocompetent cells, such as macrophages [2, 35, 41], dendritic cells [6, 35, 42], various types of T cells [5, 9, 15], and B cells/plasma cells [11], exist in large numbers in the lamina propria of the intestinal mucosa. Several of these cell types are localized in specific portions in the mucosa of the small intestine. For example, in the mouse small intestine, plasma cells are mainly located in the lower half of the intestinal villus [29], whereas TCRαβ$^+$ CD8$^+$ T cells are mainly localized in the villous epithelium, probably in a CD103/integrin alpha E-dependent manner [33]. CX3CR1$^+$ macrophages reside in whole portions of the mouse colonic lamina propria, while CD169$^+$ macrophages preferentially localize near the muscularis mucosa [2]. However, the mechanisms of localization and migration of immunocompetent cells mostly remain unclear in the small intestinal mucosa, although they have been eagerly investigated in mucosal lymphatic tissues of the intestines, such as the Peyer's patch and isolated lymphoid follicles [16, 22, 28, 32, 43].

A number of studies have reported that bacterial stimulation affects the localization and differentiation of various lymphocytes. In these studies, bacteria or bacterial components were shown to induce various effects on lymphocyte lineages *in vitro*, such as induction of proliferation and differentiation of B cells [4, 19, 30] and T cells [17, 19]. Moreover, the proliferation, differentiation

*Correspondence to: Mantani, Y.: mantani@sapphire.kobe-u.ac.jp

and localization of several lymphocyte lineages, especially IgA-producing cells [7, 10, 18, 26] and TCRαβ$^+$ CD8$^+$ intraepithelial lymphocytes [3, 12, 13, 39], have been reported to be affected by the settlement of indigenous bacteria in germ-free animals *in vivo*. These reports suggest that the localization and migration of both TCRαβ$^+$ CD8$^+$ T cells and IgA$^+$ cells are sensitive to bacteria-derived stimulation. However, the effects of indigenous bacteria on TCRαβ$^+$ CD8$^+$ T cells and IgA$^+$ cells under physiological conditions have not been investigated *in vivo*. In the rat small intestine, transient hyperproliferation of indigenous bacteria, which is observed as the expansion of bacterial colonies into the intervillous spaces, often occurs on the intestinal villus [45] and accelerates several host defenses, such as the secretion of bactericidal substances from Paneth cells [46] and acceleration of the epithelial migration [31]. However, whether such bacterial hyperproliferation affects the localization of the TCRαβ$^+$ CD8$^+$ T and IgA$^+$ B cell lineages has never been clarified. Therefore, the primary aim in the present study was to clarify the effect of the expansion of bacterial colonies into the intervillous spaces against the localization of TCRαβ$^+$ CD8$^+$ T cell and IgA$^+$ B cell lineage in the mucosa of the rat small intestine. In addition, we found that many lymphocytes, frequently with immunopositivity for L-selectin, were present in the central lymph vessel of intestinal villi in the mucosa attached to the lymphoid follicles of the Peyer's patches with bacterial colonies in the intervillous spaces in the preliminary examination, suggesting that the expansion of bacterial colonies into the intervillous spaces might induce irregular migration of L-selectin$^+$ lymphocytes in the mucosa around the Peyer's patches. Therefore, the secondary aim of the present study was to investigate the specificity of lymphocyte migration in response to the expansion of bacterial colonies into the intervillous spaces on the mucosa around the Peyer's patches with a focus on several lymphocyte lineages, including TCRαβ$^+$ CD8$^+$ T cells, IgA$^+$ B cell lineage and L-selectin$^+$ lymphocytes.

MATERIALS AND METHODS

Animals

Ten male Wistar rats aged 7 weeks (Japan SLC Inc., Hamamatsu, Japan) were maintained under specific pathogen-free conditions in individual ventilated cages (Sealsafe Plus; Tecniplast S.p.A, Buguggiate, Italy). They were permitted free access to water and food (Lab MR Stock; Nosan Corp., Yokohama, Japan). The animal facility was maintained under conditions of a 12 hr light/dark cycle (light on: 8:00 AM; light off: 20:00 PM) at 23 ± 2°C and 50 ± 10% humidity. Clinical and pathological examinations in all animals confirmed that there were no signs of disorder. This experiment was approved by the Institutional Animal Care and Use Committee (permission number: 25-06-01) and carried out according to the Kobe University Animal Experimentation Regulations.

Tissue preparation

Collection of tissues from rats was conducted from 9:00 AM to 12:00 PM. After euthanasia by overdose peritoneal injection of pentobarbital sodium (Kyoritsu Seiyaku Corp., Tokyo, Japan), tissue blocks were removed from the ileum including the Peyer's patches. Then, the tissue blocks were immersion-fixed in 4.0% paraformaldehyde fixative in 0.1 M phosphate buffer for 6 hr at 4°C, and snap-frozen in liquid nitrogen as described in a previous study [47]. Four micrometer-thick sections were cut using a Coldtome Leica CM1950 (Leica Biosystems, Nussloch, Germany), placed on slide glasses precoated with 0.2% 3-aminopropyltriethoxysilane (Shin-Etsu Chemical Co., Tokyo, Japan), and stored at −30°C until use.

Enzyme immunohistochemistry and double immunofluorescence method

Detection of antigens was conducted using the indirect method of enzyme immunohistochemical and immunofluorescence analysis with the antibodies shown in Table 1. Briefly, after rinsing with 0.05% Tween-added 0.01 M phosphate buffered saline (TPBS; pH 7.4), the sections used for the detection of all antigens except TCRαβ were heated for 20 min at 80°C for antigen retrieval. Then the sections were immersed in absolute methanol for 30 min, followed by 0.5% H_2O_2 for 30 min. After each preparation step, the sections were rinsed three times in TPBS to remove any reagent residues. After blocking with Blocking One Histo (Nacalai Tesque Inc., Kyoto, Japan) for 1 hr at room temperature (r.t.), the sections for enzyme immunohistochemical analysis were reacted with primary antibody for 18 hr at 6°C. Primary antibodies for the detection of IgA, IgG and IgM were used at considerably low concentrations in order to detect these immunoglobulins exclusively in B cells and plasma cells, and not in the interstitial fluid. The sections for the immunofluorescence analysis were reacted with one of two sets of paired antibodies—anti-L-selectin antibody/anti-TCRαβ antibody or anti-L-selectin antibody/anti-CD19 antibody—for 18 hr at 6°C. The antibody specificity for each antigen in rats is given in the respective manufacturer's manual. Then, the sections to be applied to the enzyme immunohistochemical analysis were incubated with horseradish peroxidase-conjugated secondary antibody for 1 hr at r.t. Finally, the sections for the enzyme immunohistochemical analysis were incubated with 3,3′-diaminobenzidine (Dojindo Laboratories, Mashiki, Japan) containing 0.03% H_2O_2 and counterstained with hematoxylin. The sections for immunofluorescence analysis were reacted with fluorochrome-conjugated secondary antibody and DAPI (diluted at 1:1,000; Dojindo Laboratories) for 1 hr at r.t. Control sections were incubated with TPBS or non-immunized goat IgG (Peprotech, Rocky Hill, NJ, U.S.A.) and mouse IgG (Santa Cruz Biotechnology, Santa Cruz, CA, U.S.A.) instead of the primary antibody. The sections of immunohistochemistry and double immunofluorescence were observed by Nikon Eclipse E600 Fluorescence Microscope and photographed by DS-Fi1c digital camera (Nikon, Tokyo, Japan). Fluorescence filter set B-2A, G-2A and DAPI (Nikon) were used for the observation of double immunofluorescence.

Table 1. List of antibody

	Antibody	Manufacturers	Diluted concentration	Manufacturer's specification form
Primary antibody	anti-CD8 mouse IgG	ThermoFisher Scientific, Waltham, MA, U.S.A.	1:200	MA1-70003
	anti-CD19 mouse IgG	ThermoFisher Scientific	1:100	MA5-24372
	anti-IgA goat IgG	Seikagaku Corp., Tokyo, Japan	1:20,000	270352
	anti-IgG goat IgG	Jackson ImmunoResearch Inc., West Grove, PA, U.S.A.	1:20,000	112-005-143
	anti-IgM goat IgG	Abcam, Cambridge, MA, U.S.A.	1:800	ab98365
	anti-TCRαβ mouse IgG	ThermoFisher Scientific	1:200	MA5-17541
	anti-L-selectin goat IgG	R&D Systems Inc., Minneapolis, MN, U.S.A.	1:400	AF1534
	anti-Ia mouse IgG	AbD Serotec, Oxford, U.K.	1:1,600	MCA46R
Secondary antibody	horseradish peroxidase-conjugated anti-mouse IgG rat IgG	Jackson ImmunoResearch Inc.	1:100	415-035-166
	horseradish peroxidase-conjugated anti-goat IgG donkey IgG	Jackson ImmunoResearch Inc.	1:400	705-035-147
	Rhodamine Red™-X (PRX) conjugated anti-mouse IgG rat IgG (H+L)	Jackson ImmunoResearch Inc.	1:400	415-295-166
	Alexe Fluor 488 conjugated anti-goat IgG donkey IgG	Abcam	1:400	ab150133

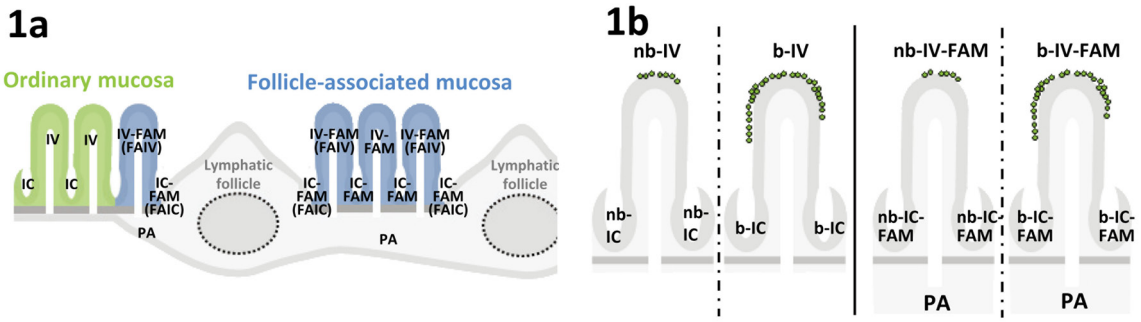

Fig. 1. a) Diagram of intestinal villus and intestinal crypt in ordinary mucosa (IV and IC) (green area) and intestinal villus and intestinal crypt in follicle-associated mucosa (IV-FAM and IC-FAM) (blue area) of the rat Peyer's patch. The dotted line represents the germinal center. b) Diagram of IV and IV-FAM without the bacterial colonies in the intervillous spaces (nb-IV and nb-IV-FAM) or with the bacterial colonies in the intervillous space (b-IV and b-IV-FAM). Green ovals on the epithelium represent indigenous bacteria. b-IC, IC adjacent to b-IV. b-IC-FAM, IC-FAM adjacent to b-IV-FAM. FAIC, follicle-associated intestinal crypt. FAIV, follicle-associated intestinal villus. nb-IC, IC adjacent to nb-IV. nb-IC-FAM, IC-FAM adjacent to nb-IV-FAM. PA, parafollicular area.

Definition of tissue elements

Sections from each tissue block were stained with hematoxylin-eosin for observation of the general structure and the expansion level of bacterial colonies. The following two types of mucosa were investigated: 1) ordinary mucosa, which were defined as mucosa without any mucosal lymphatic tissue such as Peyer's patches, isolated lymphatic follicles or cryptopatches; and 2) follicle-associated mucosa (FAM), which accompanied the parafollicular area under the muscularis mucosae in Peyer's patches in the rat ileum. Then, the intestinal villus was classified into two groups: intestinal villus in the ordinary mucosa (IV) and intestinal villus in FAM (IV-FAM), including the follicle-associated intestinal villus (FAIV), which we defined as the intestinal villus just adjacent to the lymphatic follicle in our previous study [48]. Moreover, the intestinal crypts were classified into two groups: intestinal crypts in the ordinary mucosa (IC) and intestinal crypts in FAM (IC-FAM), including follicle-associated intestinal crypts (FAIC), which we defined as intestinal crypts just adjacent to the lymphatic follicle in our previous study [48] (Fig. 1a). The intestinal villus was divided into three portions from the crypt orifice to the apex of the intestinal villus: the basal, middle and apical portions. Furthermore, IV and IV-FAM were classified into two groups based on the degree of expansion of bacterial colonies on their epithelia: nb-IV and nb-IV-FAM, in which indigenous bacteria existed only on the epithelium of the villous apex or did not exist on the epithelia at all; and b-IV and b-IV-FAM, in which the indigenous bacterial colonies were expanded from the villous apex to the intervillous space or the space between the epithelium of IV-FAM and follicle-associated epithelium. Intestinal crypts adjacent to nb-IV, b-IV, nb-IV-FAM and b-IV-FAM were defined as nb-IC, b-IC, nb-IC-FAM and b-IC-FAM, respectively (Fig. 1b). Abbreviations as defined above were listed in Table 2.

Table 2. List of abbreviations in the present study

Abbreviations related to intestinal villus		Abbreviations related to intestinal crypt	
IV	intestinal villus in ordinary mucosa	IC	intestinal crypt in ordinary mucosa
nb-IV	IV without bacterial colonies in intervillous space	nb-IC	IC adjacent to nb-IV
b-IV	IV with bacterial colonies in intervillous space	b-IC	IC adjacent to b-IV
IV-FAM	intestinal villus in follicle-associated mucosa	IC-FAM	intestinal crypt in follicle-associated mucosa
nb-IV-FAM	IV-FAM without bacterial colonies in intervillous space	nb-IC-FAM	IC-FAM adjacent to nb-IV-FAM
b-IV-FAM	IV-FAM with bacterial colonies in intervillous space	b-IC-FAM	IC-FAM adjacent to b-IV-FAM
FAIV	follicle-associated intestinal villus	FAIC	follicle-associated intestinal crypt

Histoplanimetry

For counting the number of each immunopositive cell in the epithelium and lamina propria and migrating cells in the central lymph vessel, 5 nb-IVs, b-IVs, nb-IV-FAMs and b-IV-FAMs, whose central axes were longitudinally cut, were randomly chosen from 5 rats, respectively. Then, the number of TCRαβ$^+$ and CD8$^+$ cells in the epithelium was counted in nb-IVs, b-IVs, nb-IV-FAMs and b-IV-FAMs. The number of IgA$^+$ cells per 100-μm^2 in the lamina propria was calculated in the basal, middle and apical portions of each intestinal villus and around nb-ICs, b-ICs, nb-IC-FAMs and b-IC-FAMs. The number of migrating cells per 1,000-μm^2 in the central lymph vessel, which lumen was confirmed to be located on the central axes of intestinal villus and not contained erythrocytes unlike the blood vessels, of the intestinal villus was also calculated in nb-IV, b-IV, nb-IV-FAM and b-IV-FAM using hematoxylin-eosin-stained sections. The area of the lamina propria or the central lymph vessel were determined using Image-J software (National institutes of health, Bethesda, MD, U.S.A.) to calculate the number of each cell per each unit area. Furthermore, one hundred migrating cells in the central lymph vessel of b-IV-FAM were randomly chosen from 5 rats, respectively. Then, the ratios of L-selectin$^+$, TCRαβ$^+$, CD8$^+$, CD19$^+$, IgA$^+$, IgM$^+$, IgG$^+$ and Ia$^+$ migrating cell were calculated, respectively.

Statistical analysis

The normality of distribution was first assessed by the Kolmogorov–Smirnov test. For parametric variables in multiple comparisons, two-way ANOVA was performed, followed by the Tukey–Kramer test for *post hoc* comparison. For non-parametric variables in multiple comparisons, the Kruskal–Wallis test was performed, followed by the Steel–Dwass test was performed for *post hoc* comparison.

RESULTS

The effect of bacterial colonies in the intervillous spaces against localization of CD8$^+$ T cell or IgA$^+$ B cell lineages in the rat ileum

Immunopositivity for TCRαβ was observed in the cellular membrane of the small and oval cells in ordinary mucosa and FAM (Fig. 2a). A few TCRαβ$^+$ cells were detected in the lamina propria throughout nb-IV and around nb-IC (Fig. 2b, 2c). Moreover, TCRαβ$^+$ cells were localized in the epithelium of nb-IV, but rarely detected in that of nb-IC. TCRαβ$^+$ cells in the epithelium of nb-IV were moderately detected in the basal portion and decreased toward the apical portion. These distributions of TCRαβ$^+$ cells in nb-IV and nb-IC did not differ substantially from those in b-IV and b-IC (Fig. 2b–e).

The distributions of TCRαβ$^+$ cells in nb-IV-FAM and nb-IC-FAM were similar to those in IV and IC, respectively (Fig. 2f, 2g). On the other hand, TCRαβ$^+$ cells were more abundant in the epithelium throughout b-IV-FAM, especially in apical portion, and in the lamina propria throughout b-IV-FAM and around b-IC-FAM compared with nb-IV-FAM and nb-IC-FAM, respectively (Fig. 2f–i). The number of TCRαβ$^+$ cells in the epithelium was significantly greater in b-IV-FAM than in nb-IV-FAM, and significantly greater in IV-FAM than in IV, although no significant difference was observed between the number of TCRαβ$^+$ cells in the epithelia of nb-IV and b-IV (Fig. 2j).

Immunopositivity for CD8 was observed in the cellular membrane of the small and oval cells in ordinary mucosa and FAM (Fig. 3a). CD8$^+$ cells in the lamina propria were scarce in nb-IV, b-IV and nb-IV-FAM and around nb-IC, b-IC and nb-IC-FAM, but moderately detected in b-IV-FAM and around b-IC-FAM (Fig. 3b–i). CD8$^+$ cells in the epithelium were moderately detected in the basal portion and decreased toward the apical portion in nb-IV and nb-IV-FAM (Fig. 3b, 3f). CD8$^+$ cells were more abundant in the epithelium throughout b-IV and b-IV-FAM, especially in the apical portion, compared with nb-IV and nb-IV-FAM, respectively (Fig. 3b–i), which was confirmed by histoplanimetry (Fig. 3j).

Immunopositivity for CD19, which was used as a B cell marker, was observed in the cellular membrane of the small and oval cells in FAM (Fig. 4a). In IV and IC, CD19$^+$ cells were not detected in the lamina propria regardless of the presence of bacterial colonies in the intervillous spaces (Fig. 4b, 4e). CD19$^+$ cells were also not detected in the lamina propria in nb-IV-FAM and that around nb-IC-FAM (Fig. 4c, 4f), while they were present at moderate levels in the lamina propria from the basal to middle portions of b-IV-FAM and that around b-IC-FAM (Fig. 4d, 4g).

Immunopositivities for IgA, IgM and IgG were observed in the cytoplasm of the small and oval cells in ordinary mucosa and FAM (Fig. 5a–c). IgA$^+$ cells in the lamina propria were moderately localized in the basal and middle portions and were scarce in the apical portion of nb-IV (Fig. 5d) and nb-IV-FAM (Fig. 5f) and around nb-IC (Fig. 5h) and nb-IC-FAM (Fig. 5j). On the other

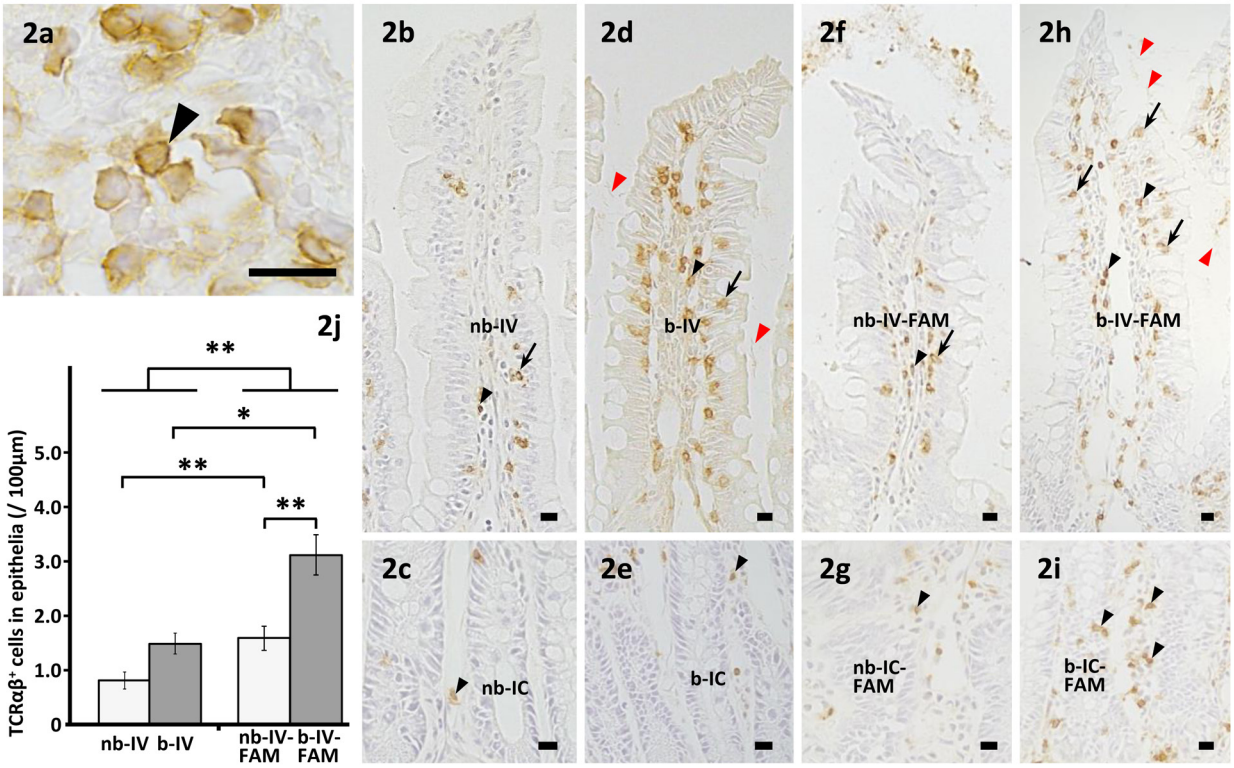

Fig. 2. Localization of TCRαβ$^+$ cells in the intestinal villus in ordinary mucosa (IV) and that in follicle-associated mucosa (FAM) (IV-FAM) and around the intestinal crypt in ordinary mucosa (IC) and that in FAM (IC-FAM). a) High magnification image of TCRαβ$^+$ cells in the lamina propria of IV. Immunopositivity for TCRαβ is observed in the cellular membrane of small and oval cells (arrowhead). b–i) TCRαβ$^+$ cells are visible in the lamina propria (black arrowheads) and epithelium (arrows) of IV or IV-FAM without bacterial colonies in the intervillous space (nb-IV (b) or nb-IV-FAM (f)) and IV or IV-FAM with bacterial colonies in the intervillous space (b-IV (d) or b-IV-FAM (h)). TCRαβ$^+$ cells in the epithelium (arrows) and lamina propria (black arrowheads) are more abundant in b-IV-FAM (h) than in nb-IV-FAM (f). TCRαβ$^+$ cells in the lamina propria (black arrowheads) are scarce around IC adjacent to nb-IV (nb-IC) (c), IC adjacent to nb-IV-FAM (nb-IC-FAM) (g) and IC adjacent to b-IV (b-IC) (e), and moderately present around IC adjacent to b-IV-FAM (b-IC-FAM) (i). Red arrowheads indicate bacterial colonies in the intervillous space. Bar=10 μm. j) The number of TCRαβ$^+$ cells in the epithelium of nb-IV, b-IV, nb-IV-FAM and b-IV-FAM per 100-μm-long epithelium. Asterisks, $P<0.05$. Double asterisks, $P<0.01$. Each value represents the mean ± SE.

hand, IgA$^+$ cells in the lamina propria were more frequent in b-IV and b-IV-FAM (Fig. 5e, 5g) and around b-IC and b-IC-FAM (Fig. 5i, 5k), compared with nb-IV, nb-IV-FAM, nb-IC and nb-IC-FAM, respectively. The number of IgA$^+$ cells in the lamina propria was significantly greater in the apical portions of b-IV and b-IV-FAM (Fig. 5l) and in the middle portions of b-IV (Fig. 5m), but not b-IV-FAM, compared with those of nb-IV and nb-IV-FAM, respectively. The numbers of IgA$^+$ cells in the lamina propria in the basal portion were not different between nb-IV and b-IV, while these numbers were smaller in b-IV-FAM than in nb-IV-FAM (Fig. 5n). IgA$^+$ cells in the lamina propria were also significantly more abundant around b-IC and b-IC-FAM compared with nb-IC and nb-IC-FAM, respectively (Fig. 5o). IgM$^+$ cells were moderately localized in the lamina propria around the IC and the lamina propria of the basal portion of IV, and were decreased toward the lamina propria of the apical portion of IV (Fig. 5p, 5q). IgM$^+$ cells in the lamina propria were more frequently detected in IV-FAM and around IC-FAM than IV and IC, respectively (Fig. 5r, 5s). IgG$^+$ cells were scarcely detected in the lamina propria of IV, IC, IV-FAM and IC-FAM (Fig. 5t). The above findings on IgM and IgG were similar regardless of the presence of bacterial colonies in the intervillous spaces of IV and IV-FAM.

The effect of bacterial colonies in the intervillous spaces against localization of L-selectin$^+$ lymphocytes in rat ileum

Migrating cells were frequently accumulated in the central lymph vessel of b-IV-FAM, but were rarely accumulated in those of nb-IV, b-IV and nb-IV-FAM (Fig. 6a, 6b). The migrating cells were significantly more abundant in the central lymph vessel of b-IV-FAM than in those of nb-IV, b-IV or nb-IV-FAM, while the levels of migrating cells in the central lymph vessel were not significantly different between nb-IV and b-IV (Fig. 6c). Migrating cells in the central lymph vessel of b-IV-FAM were immunopositive for L-selectin (94.4 ± 1.60%), TCRαβ (58.6 ± 2.29%), CD8 (26.2 ± 1.11%), CD19 (28.2 ± 0.86%), IgA (2.8 ± 0.86%), IgM (30.2 ± 2.59%), IgG (3.2 ± 1.06%) and Ia (29.6 ± 2.04%) (Fig. 6d–k).

L-selectin$^+$ cells were not detected in the lamina propria of IV or the lamina propria around IC regardless of the presence of bacterial colonies in the intervillous spaces of IV (Fig. 7a, 7b), although in rare cases they were detected in the central lymph vessel of IV regardless of the presence of bacterial colonies in the intervillous spaces of IV. Small numbers of L-selectin$^+$ cells

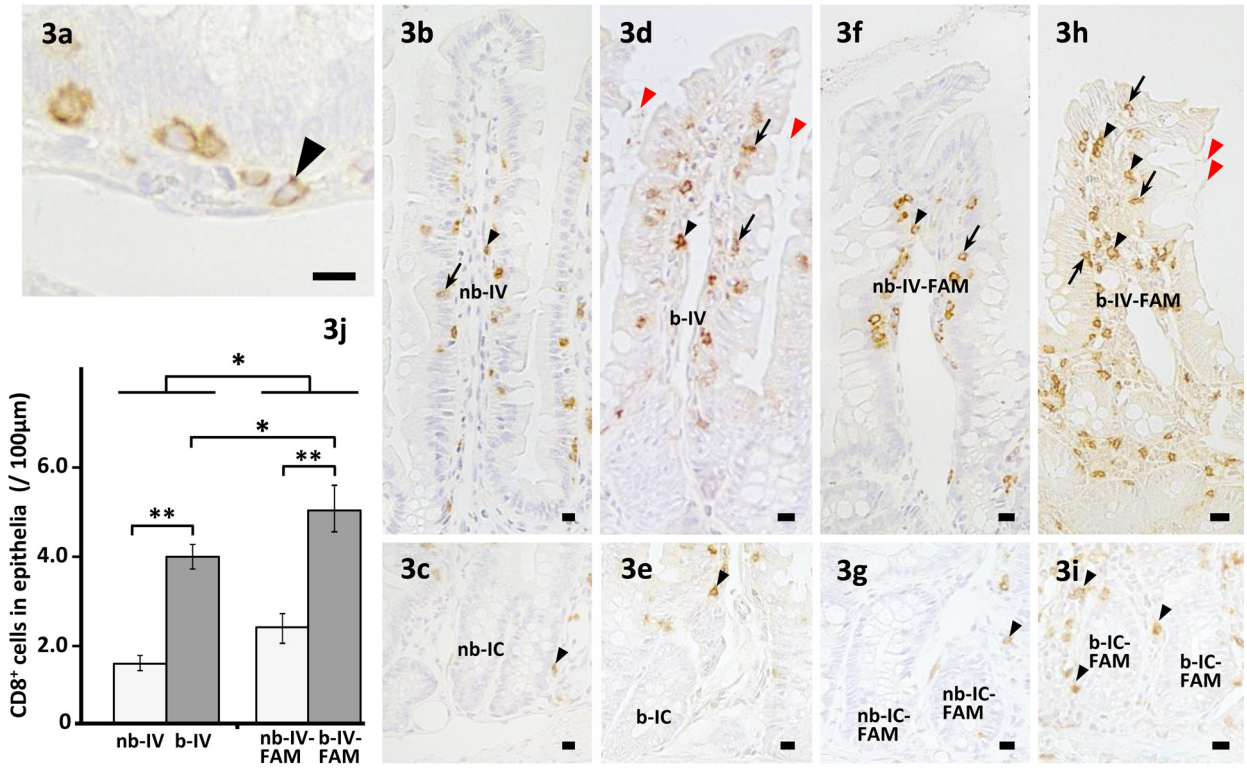

Fig. 3. Localization of $CD8^+$ cells in the intestinal villus in ordinary mucosa (IV) and that in follicle-associated mucosa (FAM) (IV-FAM) and around the intestinal crypt in ordinary mucosa (IC) and that in FAM (IC-FAM). a) High magnification image of $CD8^+$ cells in the lamina propria and epithelium of IV. Immunopositivity for CD8 is observed in cellular membrane of small and oval cells (arrowhead). b–i) $CD8^+$ cells are visible in the lamina propria (black arrowheads) and epithelium (arrows) of IV or IV-FAM without bacterial colonies in the intervillous space (nb-IV (b) or nb-IV-FAM (f)) and IV or IV-FAM with bacterial colonies in the intervillous space (b-IV (d) or b-IV-FAM (h)). $CD8^+$ cells in the lamina propria (black arrowheads) are scarce in nb-IV (b), b-IV (d) and nb-IV-FAM (f), and moderately present in b-IV-FAM (h). $CD8^+$ cells in the epithelium (arrows) are more abundant in b-IV (d) and b-IV-FAM (h) compared with nb-IV (b) and nb-IV-FAM (f), respectively. $CD8^+$ cells in the lamina propria (black arrowheads) are scarce around IC adjacent to nb-IV (nb-IC) (c), IC adjacent to b-IV (b-IC) (e) and IC adjacent to nb-IV-FAM (nb-IC-FAM) (g), and moderately present around IC adjacent to b-IV-FAM (b-IC-FAM) (i). Red arrowheads indicate bacterial colonies in the intervillous space. Bar=10 μm. j) The number of $CD8^+$ cells in a 100-μm segment of the epithelium of nb-IV, nb-IV-FAM, b-IV and b-IV-FAM. Asterisks, $P<0.05$. Double asterisks, $P<0.01$. Each value represents the mean ± SE.

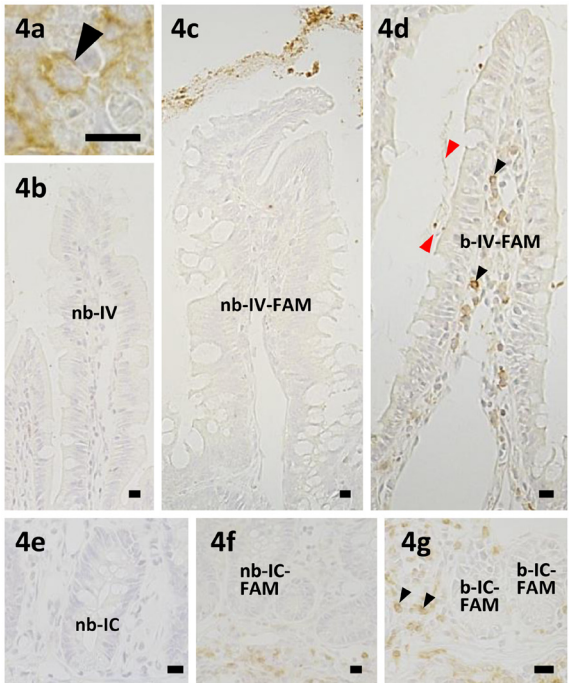

Fig. 4. Localization of $CD19^+$ cells in the intestinal villus in ordinary mucosa (IV) and that in follicle-associated mucosa (FAM) (IV-FAM) and around the intestinal crypt in ordinary mucosa (IC) and that in FAM (IC-FAM). a) High magnification image of $CD19^+$ cells in the lamina propria of IV-FAM. Immunopositivity for CD19 is observed in the cellular membrane of small and oval cells (arrowhead). b–g) $CD19^+$ cells (black arrowheads) are visible in the lamina propria of IV-FAM with bacterial colonies in the intervillous space (b-IV-FAM) (d) and that around IC-FAM adjacent to b-IV-FAM (b-IC-FAM) (g), but not in the lamina propria of IV or IV-FAM without bacterial colonies in the intervillous spaces (nb-IV (b) or nb-IV-FAM (c)) and around IC adjacent to nb-IV (nb-IC) (e) or nb-IV-FAM (nb-IC-FAM) (f). Red arrowheads indicate bacterial colonies in the intervillous space. Bar=10 μm.

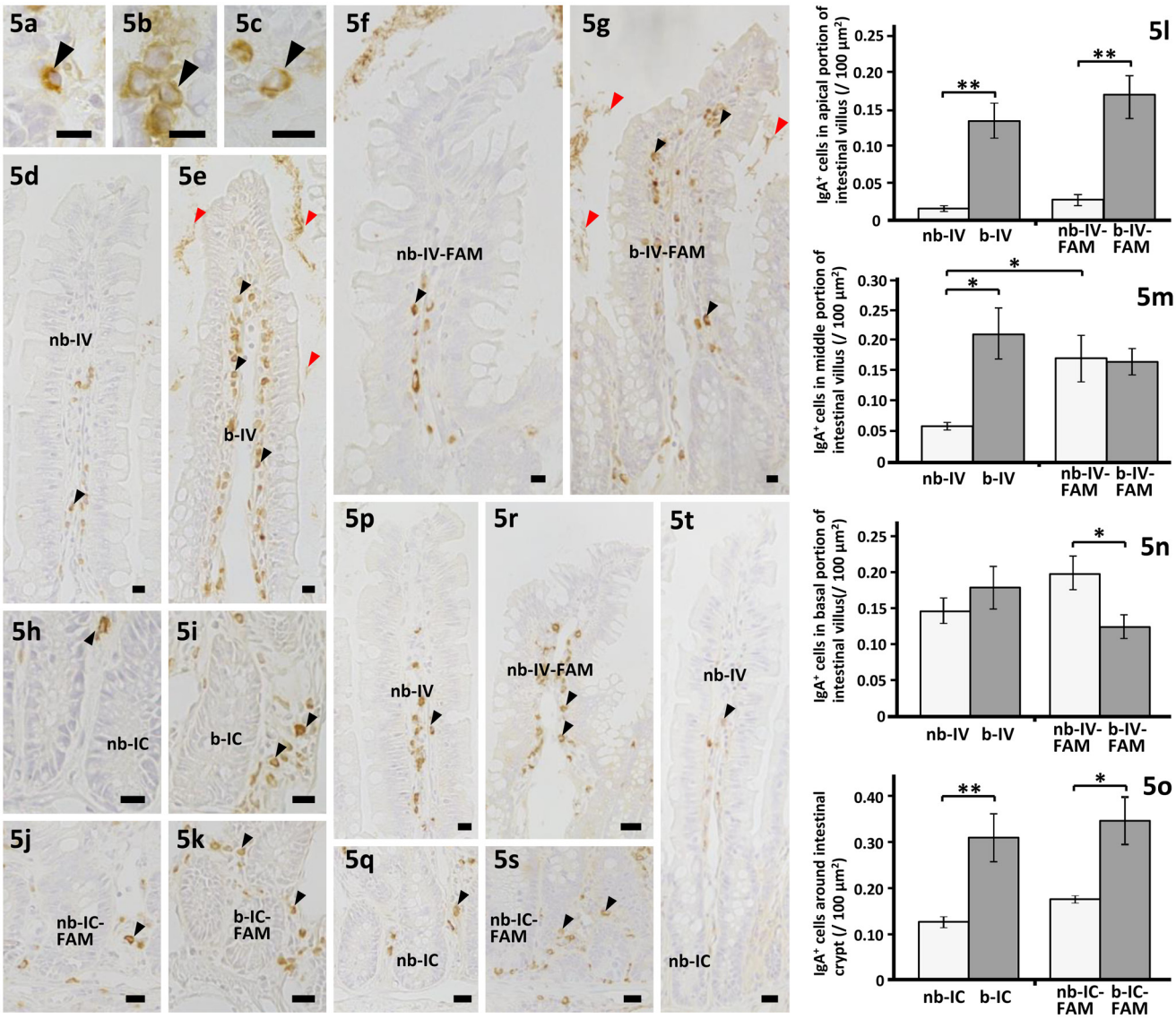

Fig. 5. Localization of IgA$^+$, IgM$^+$ and IgG$^+$ cells in the intestinal villus in ordinary mucosa (IV) and that in follicle-associated mucosa (FAM) (IV-FAM) and around the intestinal crypt in ordinary mucosa (IC) and that in FAM (IC-FAM). a–c) High magnification image of IgA$^+$ (a), IgM$^+$ (b) and IgG$^+$ cells (c) in the lamina propria of IV. Immunopositivity for IgA, IgM or IgG is observed in the cytoplasm of small and oval cells in IV (arrowhead). d–k) IgA$^+$ cells (black arrowheads) are visible in the lamina propria of IV or IV-FAM without bacterial colonies in the intervillous space (nb-IV (d) or nb-IV-FAM (f)) and IV or IV-FAM with bacterial colonies in the intervillous space (b-IV (e) or b-IV-FAM (g)) and the lamina propria around IC adjacent to b-IV (b-IC) (i) and IC adjacent to b-IV-FAM (b-IC-FAM) (k), but scarce around IC adjacent to nb-IV (nb-IC) (h) and IC adjacent to nb-IV-FAM (nb-IC-FAM) (j). IgA$^+$ cells are visible in the basal and middle portions of nb-IV (d) and nb-IV-FAM (f), but are visible in the entirety of b-IV (e) and b-IV-FAM (g). Red arrowheads indicate bacterial colonies in the intervillous space. l–o) The number of IgA$^+$ cells per 100-μm^2 in the lamina propria of the apical (l), middle (m) and basal portions (n) of nb-IV, nb-IV-FAM, b-IV and b-IV-FAM and that around nb-IC, nb-IC-FAM, b-IC, and b-IC-FAM (o). Asterisks, P<0.05. Double asterisks, P<0.01. Each value represents the mean ± SE. p–s) IgM$^+$ cells (arrowheads) are visible in the lamina propria of nb-IV (p) and nb-IV-FAM (r) and that around nb-IC (q) and nb-IC-FAM (s), with IgM$^+$ cells being abundant in nb-IV-FAM and nb-IC-FAM. t) IgG$^+$ cells (arrowhead) are scarce in the lamina propria of nb-IV and that around nb-IC. Bar=10 μm.

were detected in the lamina propria around nb-IC-FAM, but L-selectin$^+$ cells were scarce in nb-IV-FAM (Fig. 7c, 7d). On the other hand, L-selectin$^+$ cells were frequently found in the lamina propria of b-IV-FAM and that around b-IC-FAM. Moreover, L-selectin$^+$ cells were often continuously distributed from the parafollicular area of Peyer's patch to the lamina propria around b-IC-FAM, and occasionally expanded into the middle portion of b-IV-FAM (Fig. 7e, 7f). Double immunofluorescence for L-selectin and TCRαβ or CD19 showed that L-selectin$^+$ cells from the parafollicular area to IV-FAM were frequently immunopositive for TCRαβ$^+$ (Fig. 7g) and occasionally immunopositive for CD19 (Fig. 7h). Co-localizations of L-selectin/TCRαβ or CD19 were also found in the migrating cells in the central lymph vessel of b-IV-FAM.

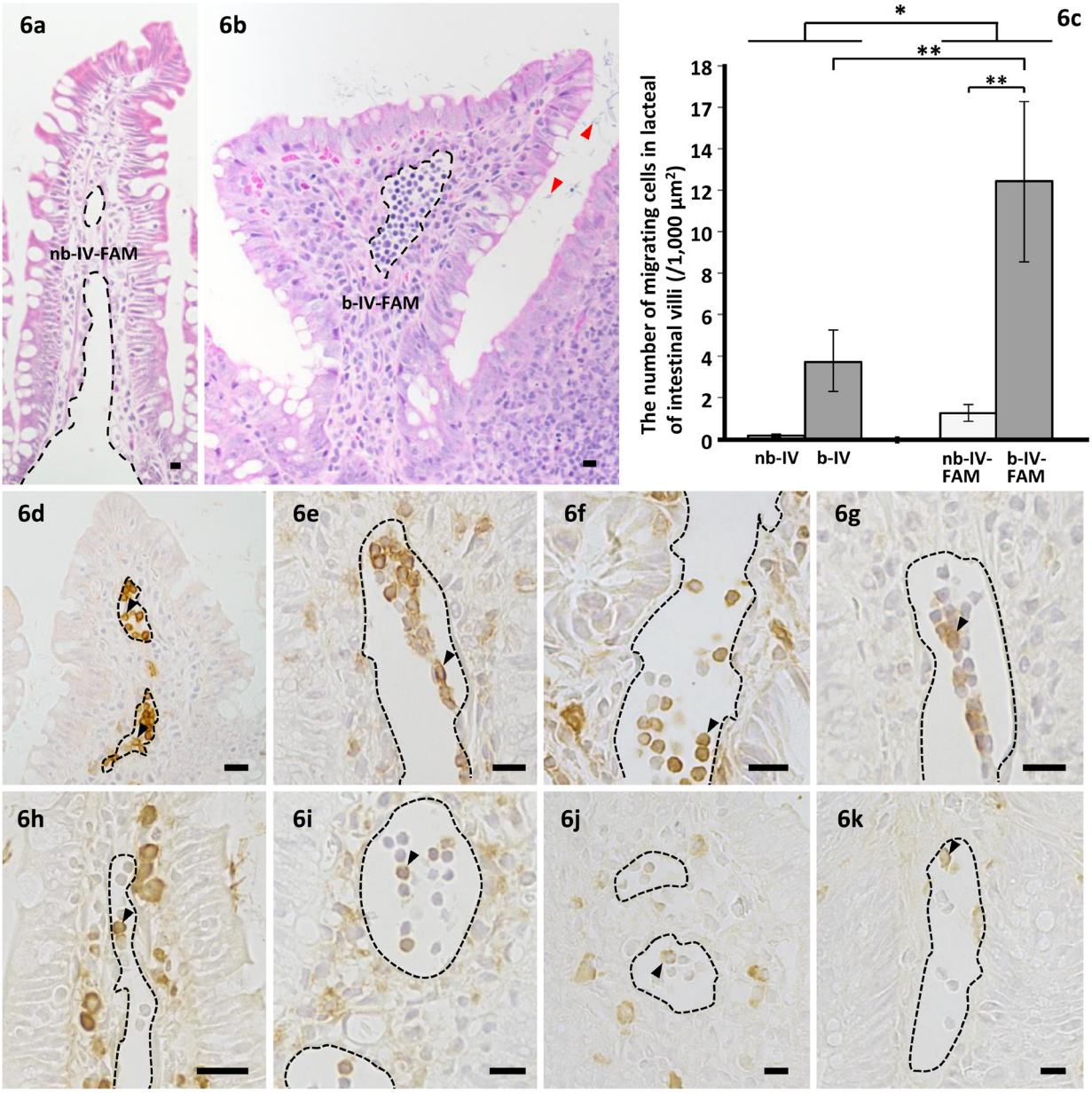

Fig. 6. Migrating cells in the central lymph vessel of the intestinal villus in ordinary mucosa (IV) and that in follicle-associated mucosa (IV-FAM). a, b) Migrating cells are not visible in the central lymph vessel of IV-FAM without bacterial colonies in the intervillous space (nb-IV-FAM) (a), but are abundantly visible in the central lymph vessel of IV-FAM with bacterial colonies in the intervillous space (b-IV-FAM) (b). Red arrowheads indicate bacterial colonies in the intervillous space. c) The number of migrating cells per 1,000-μm^2 in the central lymph vessel of IV without bacterial colonies in the intervillous space (nb-IV), IV with bacterial colonies in the intervillous space (b-IV), nb-IV-FAM and b-IV-FAM. Asterisks, P<0.05. Double asterisks, P<0.01. Each value represents the mean ± SE. d–k) Immunopositivity for each cellular marker in the migrating cells in the central lymph vessel of b-IV-FAM. Migrating cells in the central lymph vessel of b-IV-FAM are immunopositive (arrowheads) for L-selectin (d), TCRαβ (e), CD8 (f), CD19 (g), IgA (h), IgM (i), IgG (j) and Ia (k). Dashed lines, central lymph vessel. Bar=10 μm.

The changes of histological localization of several lymphocyte lineages in response to the expansion of bacterial colonies into the intervillous spaces are summarized in Fig. 8.

DISCUSSION

TCRαβ$^+$ CD8$^+$ intraepithelial lymphocytes reside in the intestinal epithelium of the mouse small intestine, likely in CD103/integrin alpha E-dependent manner [33]. The number and activity of TCRαβ$^+$ intraepithelial lymphocytes have been reported to increase in mice with monoassociation of segmented filamentous bacteria compared with germ-free mice [37, 38]. In the present

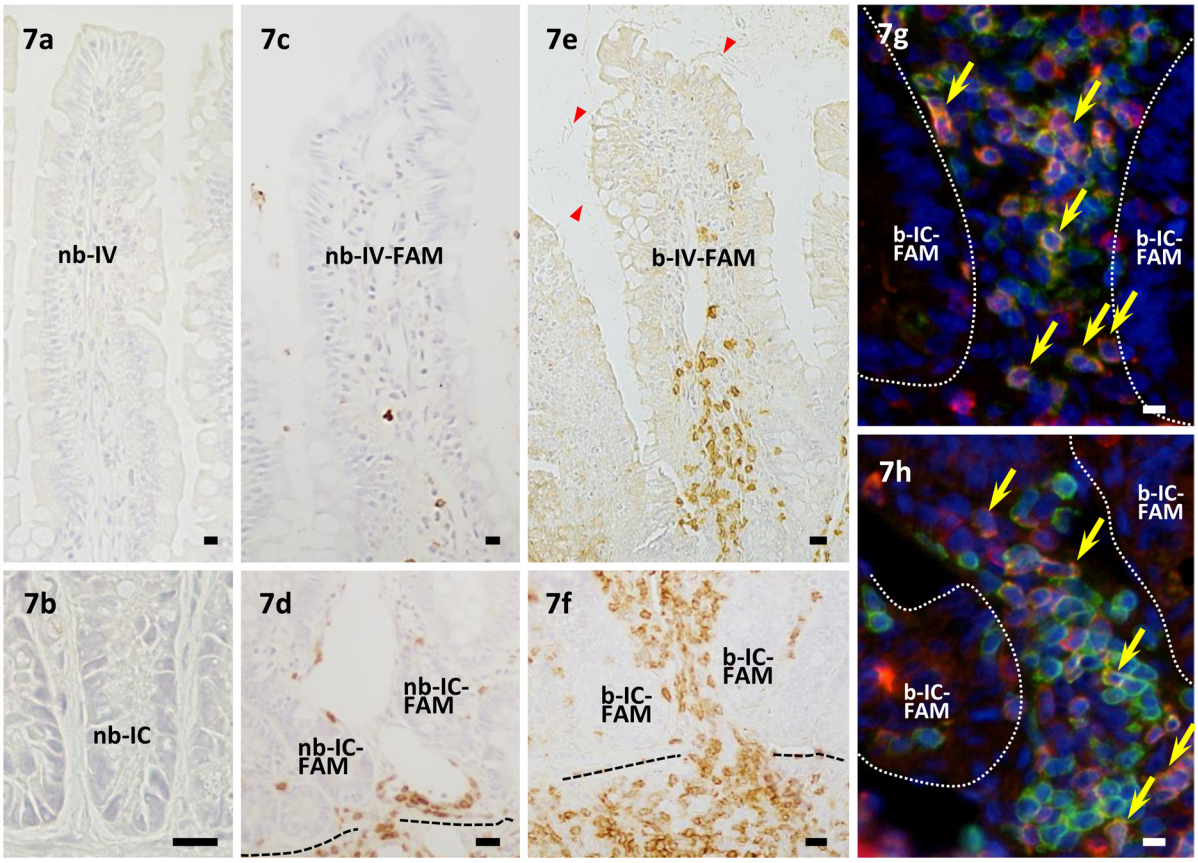

Fig. 7. Localization of L-selectin$^+$ cells in the intestinal villus in ordinary mucosa (IV) and that in follicle-associated mucosa (FAM) (IV-FAM) and around the intestinal crypt in ordinary mucosa (IC) and that in FAM (IC-FAM). a, b) Immunopositivity for L-selectin is not visible in the lamina propria of IV without bacterial colonies in the intervillous space (nb-IV) (a) and IC adjacent to nb-IV (nb-IC) (b). c–f) L-selectin$^+$ cells are scarce in the lamina propria of IV-FAM without bacterial colonies in the intervillous space (nb-IV-FAM) (c) and that around IC adjacent to nb-IV-FAM (nb-IC-FAM) (d), but are abundant in that of IV-FAM with bacterial colonies in the intervillous space (b-IV-FAM) (e) and that around IC adjacent to b-IV-FAM (b-IC-FAM) (f). L-selectin$^+$ cells are continuously distributed from the parafollicular area to the lamina propria around b-IC-FAM (f). Red arrowheads indicate bacterial colonies in the intervillous space. g, h) Double immunofluorescence against L-selectin (green)/TCRαβ (red) (g) and L-selectin (green)/CD19 (red) (h) in the lamina propria around b-IC-FAM. Co-localizations of L-selectin/TCRαβ (g) or CD19 (h) (yellow arrows) are visible in the lamina propria around b-IC-FAM. Dotted lines represent the basal membrane of the epithelium. Bar=10 μm.

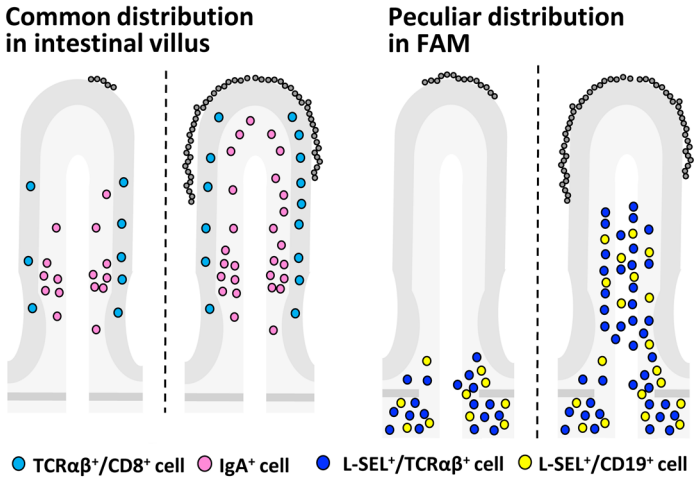

Fig. 8. Schematic diagram of localization of the lymphocyte lineage in the ordinary mucosa and follicle-associated mucosa (FAM). Gray ovals on the epithelium represent indigenous bacteria.

study, the numbers of TCRαβ$^+$ or CD8$^+$ cells were increased in the epithelia of the intestinal villi of the ordinary mucosa and FAM in response to the expansion of bacterial colonies into the intervillous spaces in the rat ileum. These findings suggest that the number of TCRαβ$^+$ CD8$^+$ T cells in the villous epithelium could be affected even by transient proliferation of indigenous bacteria. Intraepithelial lymphocytes have been suggested to contribute to the formation of an intestinal epithelial barrier against bacterial invasion in various ways. For example, intraepithelial lymphocytes are suggested to promote the expression of claudin-1 by epithelial cells and increase mucus thickness in response to bacterial stimulation [21]. In addition, intraepithelial lymphocytes are suggested to produce bactericidal lectin RegIIIβ in response to bacterial stimulation [14]. Therefore, an increase of intraepithelial lymphocytes in response to the expansion of bacterial colonies into the intervillous spaces might contribute to the enhancement of local intestinal epithelial intensity and secretory host defense mediated by the mucus and innate antimicrobial factors against proliferating bacteria under physiological conditions.

Monoassociation of segmented filamentous bacteria in germ-free mice has been shown to increase the number of IgA-producing cells in the lamina propria [38]. Bacterial stimulation has been suggested to increase IgA$^+$ cells in the lamina propria and fecal IgA in the mouse small intestine [34]. In the present study, IgA$^+$ cells possessed IgA-immunopositivity in their cytoplasms and changed their localization in response to the expansion of bacterial colonies into the intervillous spaces of IV and IV-FAM, while the localizations of IgG$^+$, IgM$^+$ and CD19$^+$ cells were not changed and thus did not correspond with the change of localization of IgA$^+$ cells in response to the expansion of bacterial colonies. CD19 is expressed in murine and human pro-B cells, pre-B cells and B cells, but not plasma cells [20]. These findings suggest that the IgA$^+$ cells that changed their localization in response to the expansion of bacterial colonies into the intervillous spaces in the present study were plasma cells. IgA are secreted from the intestinal crypt [27], coat the indigenous bacteria in the feces [40] and inhibit the bacterial adherence on the mucosal epithelium [44]. Based on these previous findings, our present result suggests that IgA$^+$ cells, probably plasma cells, were increased around the intestinal crypt in response to the expansion of bacterial colonies into the intervillous spaces and contribute to the local host defenses against the indigenous bacteria on the epithelium of intestinal villi. In addition, IgA$^+$ cells increased not only around the intestinal crypt, but also in the apical portions of IV and IV-FAM in response to the expansion of bacterial colonies into the intervillous spaces. Lipopolysaccharide, one of the Gram-negative bacterial constituents, is absorbed from the intestine into the blood stream in humans even under healthy conditions [1], and this process is accelerated during the postprandial period by a high-fat diet [8]. Intestinal IgA have been shown to bind lipopolysaccharide from indigenous bacteria [23]. Considering that Gram-negative bacteria are more abundant in deep portions of intervillous spaces of the rat small intestine than Gram-positive bacteria [24], an increase of IgA$^+$ cells—probably plasma cells—in the apical portion of the intestinal villus in response to the expansion of bacterial colonies into the intervillous spaces might contribute to the protection against or neutralization of absorbed bacterial constituents such as lipopolysaccharide from Gram-negative bacteria.

Most of the studies on Peyer's patches have concentrated on the characteristics of the lymphatic follicle. However, we previously reported that the FAIV, which is the intestinal villus just adjacent to the lymphatic follicle and is included in the IV-FAM, have special mechanism for recognition of bacteria [48], and that the follicle-associated intestinal crypts, which are included in the IC-FAM, have an unusual composition of epithelial cells [25] in the rat Peyer's patches. In the present study, L-selectin$^+$ cells, which also express TCRαβ or CD19, were numerously detected in the central lymph vessel of b-IV-FAM, although migrating cells themselves were rarely detected in the central lymph vessel even in nb-IV, b-IV and nb-IV-FAM. In addition, L-selectin$^+$ cells were continuously localized from the parafollicular area to the lamina propria of the middle portion of b-IV-FAM and were immunopositive for TCRαβ or CD19. These findings suggest that L-selectin$^+$ B cells and T cells migrate from the parafollicular area of Peyer's patches to the lamina propria of IV-FAM and enter the central lymph vessel of IV-FAM in response to the expansion of bacterial colonies into the intervillous spaces of the IV-FAM, although the host defenses against indigenous bacteria by CD8$^+$ T cell and IgA$^+$ B cell lineages were probably common in both the ordinary mucosa and FAM. It has been clarified that lymph vessel of mesentery from area with Peyer's patches include more abundant migrating cells than that from area without Peyer's patches in rat small intestine [36]. From these findings, the expansion of bacterial colonies into the intervillous spaces might induce the active replacement of T and B cells in IV-FAM and abundant supplementations of the lymphocyte toward the mesenteric lymph nodes from IV-FAM in the rat ileum, and these actions could contribute to the effective induction of an immune response. This peculiar migration of lymphocytes in IV-FAM suggest the existence of specific signals for chemotaxis, which could regulate the migration of lymphocytes, in the FAM. In the future, the expression of chemokines and its receptor and the peculiar intracellular communication among various immunocompetent cells in IV-FAM is needed to be investigated.

ACKNOWLEDGMENT. This work was financially supported in part by a Grant-in-Aid for Scientific Research (nos. 15K07766 and 16K18813) from the Japan Society for the Promotion of Science.

REFERENCES

1. Amar, J., Burcelin, R., Ruidavets, J. B., Cani, P. D., Fauvel, J., Alessi, M. C., Chamontin, B. and Ferriéres, J. 2008. Energy intake is associated with endotoxemia in apparently healthy men. *Am. J. Clin. Nutr.* **87**: 1219–1223. [Medline] [CrossRef]
2. Asano, K., Takahashi, N., Ushiki, M., Monya, M., Aihara, F., Kuboki, E., Moriyama, S., Iida, M., Kitamura, H., Qiu, C. H., Watanabe, T. and Tanaka, M. 2015. Intestinal CD169(+) macrophages initiate mucosal inflammation by secreting CCL8 that recruits inflammatory monocytes. *Nat. Commun.* **6**: 7802. [Medline] [CrossRef]
3. Bandeira, A., Mota-Santos, T., Itohara, S., Degermann, S., Heusser, C., Tonegawa, S. and Coutinho, A. 1990. Localization of gamma/delta T cells to

the intestinal epithelium is independent of normal microbial colonization. *J. Exp. Med.* **172**: 239–244. [Medline] [CrossRef]
4. Bernasconi, N. L., Onai, N. and Lanzavecchia, A. 2003. A role for Toll-like receptors in acquired immunity: up-regulation of TLR9 by BCR triggering in naive B cells and constitutive expression in memory B cells. *Blood* **101**: 4500–4504. [Medline] [CrossRef]
5. Bjerke, K., Brandtzaeg, P. and Fausa, O. 1988. T cell distribution is different in follicle-associated epithelium of human Peyer's patches and villous epithelium. *Clin. Exp. Immunol.* **74**: 270–275. [Medline]
6. Bogunovic, M., Ginhoux, F., Helft, J., Shang, L., Hashimoto, D., Greter, M., Liu, K., Jakubzick, C., Ingersoll, M. A., Leboeuf, M., Stanley, E. R., Nussenzweig, M., Lira, S. A., Randolph, G. J. and Merad, M. 2009. Origin of the lamina propria dendritic cell network. *Immunity* **31**: 513–525. [Medline] [CrossRef]
7. Crabbé, P. A., Bazin, H., Eyssen, H. and Heremans, J. F. 1968. The normal microbial flora as a major stimulus for proliferation of plasma cells synthesizing IgA in the gut. The germ-free intestinal tract. *Int. Arch. Allergy Appl. Immunol.* **34**: 362–375. [Medline] [CrossRef]
8. Erridge, C., Attina, T., Spickett, C. M. and Webb, D. J. 2007. A high-fat meal induces low-grade endotoxemia: evidence of a novel mechanism of postprandial inflammation. *Am. J. Clin. Nutr.* **86**: 1286–1292. [Medline] [CrossRef]
9. Hadis, U., Wahl, B., Schulz, O., Hardtke-Wolenski, M., Schippers, A., Wagner, N., Müller, W., Sparwasser, T., Förster, R. and Pabst, O. 2011. Intestinal tolerance requires gut homing and expansion of FoxP3$^+$ regulatory T cells in the lamina propria. *Immunity* **34**: 237–246. [Medline] [CrossRef]
10. Hapfelmeier, S., Lawson, M. A., Slack, E., Kirundi, J. K., Stoel, M., Heikenwalder, M., Cahenzli, J., Velykoredko, Y., Balmer, M. L., Endt, K., Geuking, M. B., Curtiss, R. 3rd., McCoy, K. D. and Macpherson, A. J. 2010. Reversible microbial colonization of germ-free mice reveals the dynamics of IgA immune responses. *Science* **328**: 1705–1709. [Medline] [CrossRef]
11. He, B., Xu, W., Santini, P. A., Polydorides, A. D., Chiu, A., Estrella, J., Shan, M., Chadburn, A., Villanacci, V., Plebani, A., Knowles, D. M., Rescigno, M. and Cerutti, A. 2007. Intestinal bacteria trigger T cell-independent immunoglobulin A(2) class switching by inducing epithelial-cell secretion of the cytokine APRIL. *Immunity* **26**: 812–826. [Medline] [CrossRef]
12. Helgeland, L., Dissen, E., Dai, K. Z., Midtvedt, T., Brandtzaeg, P. and Vaage, J. T. 2004. Microbial colonization induces oligoclonal expansions of intraepithelial CD8 T cells in the gut. *Eur. J. Immunol.* **34**: 3389–3400. [Medline] [CrossRef]
13. Imaoka, A., Matsumoto, S., Setoyama, H., Okada, Y. and Umesaki, Y. 1996. Proliferative recruitment of intestinal intraepithelial lymphocytes after microbial colonization of germ-free mice. *Eur. J. Immunol.* **26**: 945–948. [Medline] [CrossRef]
14. Ismail, A. S., Severson, K. M., Vaishnava, S., Behrendt, C. L., Yu, X., Benjamin, J. L., Ruhn, K. A., Hou, B., DeFranco, A. L., Yarovinsky, F. and Hooper, L. V. 2011. Gammadelta intraepithelial lymphocytes are essential mediators of host-microbial homeostasis at the intestinal mucosal surface. *Proc. Natl. Acad. Sci. U.S.A.* **108**: 8743–8748. [Medline] [CrossRef]
15. Ivanov, I. I., Atarashi, K., Manel, N., Brodie, E. L., Shima, T., Karaoz, U., Wei, D., Goldfarb, K. C., Santee, C. A., Lynch, S. V., Tanoue, T., Imaoka, A., Itoh, K., Takeda, K., Umesaki, Y., Honda, K. and Littman, D. R. 2009. Induction of intestinal Th17 cells by segmented filamentous bacteria. *Cell* **139**: 485–498. [Medline] [CrossRef]
16. Iwasaki, A. and Kelsall, B. L. 2000. Localization of distinct Peyer's patch dendritic cell subsets and their recruitment by chemokines macrophage inflammatory protein (MIP)-3α, MIP-3β, and secondary lymphoid organ chemokine. *J. Exp. Med.* **191**: 1381–1394. [Medline] [CrossRef]
17. Keppler, S. J., Theil, K., Vucikuja, S. and Aichele, P. 2009. Effector T-cell differentiation during viral and bacterial infections: Role of direct IL-12 signals for cell fate decision of CD8$^+$ T cells. *Eur. J. Immunol.* **39**: 1774–1783. [Medline] [CrossRef]
18. Klaasen, H. L., Van der Heijden, P. J., Stok, W., Poelma, F. G., Koopman, J. P., Van den Brink, M. E., Bakker, M. H., Eling, W. M. and Beynen, A. C. 1993. Apathogenic, intestinal, segmented, filamentous bacteria stimulate the mucosal immune system of mice. *Infect. Immun.* **61**: 303–306. [Medline]
19. Koch, R. J. and Brodsky, L. 1993. Effect of specific bacteria on lymphocyte proliferation in diseased and nondiseased tonsils. *Laryngoscope* **103**: 1020–1026. [Medline] [CrossRef]
20. Kozmik, Z., Wang, S., Dörfler, P., Adams, B. and Busslinger, M. 1992. The promoter of the CD19 gene is a target for the B-cell-specific transcription factor BSAP. *Mol. Cell. Biol.* **12**: 2662–2672. [Medline] [CrossRef]
21. Kuhn, K. A., Schulz, H. M., Regner, E. H., Severs, E. L., Hendrickson, J. D., Mehta, G., Whitney, A. K., Ir, D., Ohri, N., Robertson, C. E., Frank, D. N., Campbell, E. L. and Colgan, S. P. 2018. Bacteroidales recruit IL-6-producing intraepithelial lymphocytes in the colon to promote barrier integrity. *Mucosal Immunol.* **11**: 357–368. [Medline] [CrossRef]
22. Lian, J. and Luster, A. D. 2015. Chemokine-guided cell positioning in the lymph node orchestrates the generation of adaptive immune responses. *Curr. Opin. Cell Biol.* **36**: 1–6. [Medline] [CrossRef]
23. Macpherson, A. J., Gatto, D., Sainsbury, E., Harriman, G. R., Hengartner, H. and Zinkernagel, R. M. 2000. A primitive T cell-independent mechanism of intestinal mucosal IgA responses to commensal bacteria. *Science* **288**: 2222–2226. [Medline] [CrossRef]
24. Mantani, Y., Yokoo, Y., Kamezaki, A., Udayanga, K. G. S., Takahara, E., Takeuchi, T., Kawano, J., Yokoyama, T., Hoshi, N. and Kitagawa, H. 2012. Immunohistochemical detection of toll-like receptor-2, -4 and -9 in exocrine glands associated with rat alimentary tract. *J. Vet. Med. Sci.* **74**: 1429–1438. [Medline] [CrossRef]
25. Mantani, Y., Yuasa, H., Nishida, M., Takahara, E., Omotehara, T., Udayanga, K. G. S., Kawano, J., Yokoyama, T., Hoshi, N. and Kitagawa, H. 2014. Peculiar composition of epithelial cells in follicle-associated intestinal crypts of Peyer's patches in the rat small intestine. *J. Vet. Med. Sci.* **76**: 833–838. [Medline] [CrossRef]
26. Moreau, M. C., Ducluzeau, R., Guy-Grand, D. and Muller, M. C. 1978. Increase in the population of duodenal immunoglobulin A plasmocytes in axenic mice associated with different living or dead bacterial strains of intestinal origin. *Infect. Immun.* **21**: 532–539. [Medline]
27. O'Daly, J. A., Craig, S. W. and Cebra, J. J. 1971. Localization of b markers, α-chain and SC of SIgA in epithelial cells lining Lieberkühn crypts. *J. Immunol.* **106**: 286–288. [Medline]
28. Okada, T., Ngo, V. N., Ekland, E. H., Förster, R., Lipp, M., Littman, D. R. and Cyster, J. G. 2002. Chemokine requirements for B cell entry to lymph nodes and Peyer's patches. *J. Exp. Med.* **196**: 65–75. [Medline] [CrossRef]
29. Pabst, O., Ohl, L., Wendland, M., Wurbel, M. A., Kremmer, E., Malissen, B. and Förster, R. 2004. Chemokine receptor CCR9 contributes to the localization of plasma cells to the small intestine. *J. Exp. Med.* **199**: 411–416. [Medline] [CrossRef]
30. Pardo, I., Carafa, C., Dziarski, R. and Levinson, A. I. 1984. Analysis of in vitro polyclonal B cell differentiation responses to bacterial peptidoglycan and pokeweed mitogen in rheumatoid arthritis. *Clin. Exp. Immunol.* **56**: 253–262. [Medline]
31. Qi, W. M., Yamamoto, K., Yokoo, Y., Miyata, H., Inamoto, T., Udayanga, K. G. S., Kawano, J., Yokoyama, T., Hoshi, N. and Kitagawa, H. 2009. Histoplanimetrical study on the relationship between the cell kinetics of villous columnar epithelial cells and the proliferation of indigenous bacteria in rat small intestine. *J. Vet. Med. Sci.* **71**: 463–470. [Medline] [CrossRef]
32. Schmidt, T. H., Bannard, O., Gray, E. E. and Cyster, J. G. 2013. CXCR4 promotes B cell egress from Peyer's patches. *J. Exp. Med.* **210**: 1099–1107. [Medline] [CrossRef]

33. Schön, M. P., Arya, A., Murphy, E. A., Adams, C. M., Strauch, U. G., Agace, W. W., Marsal, J., Donohue, J. P., Her, H., Beier, D. R., Olson, S., Lefrancois, L., Brenner, M. B., Grusby, M. J. and Parker, C. M. 1999. Mucosal T lymphocyte numbers are selectively reduced in integrin α E (CD103)-deficient mice. *J. Immunol.* **162**: 6641–6649. [Medline]
34. Shang, L., Fukata, M., Thirunarayanan, N., Martin, A. P., Arnaboldi, P., Maussang, D., Berin, C., Unkeless, J. C., Mayer, L., Abreu, M. T. and Lira, S. A. 2008. Toll-like receptor signaling in small intestinal epithelium promotes B-cell recruitment and IgA production in lamina propria. *Gastroenterology* **135**: 529–538. [Medline] [CrossRef]
35. Soesatyo, M., Biewenga, J., Kraal, G. and Sminia, T. 1990. The localization of macrophage subsets and dendritic cells in the gastrointestinal tract of the mouse with special reference to the presence of high endothelial venules. An immuno- and enzyme-histochemical study. *Cell Tissue Res.* **259**: 587–593. [Medline] [CrossRef]
36. Steer, H. W. 1980. An analysis of the lymphocyte content of rat lacteals. *J. Immunol.* **125**: 1845–1848. [Medline]
37. Umesaki, Y., Okada, Y., Matsumoto, S., Imaoka, A. and Setoyama, H. 1995. Segmented filamentous bacteria are indigenous intestinal bacteria that activate intraepithelial lymphocytes and induce MHC class II molecules and fucosyl asialo GM1 glycolipids on the small intestinal epithelial cells in the ex-germ-free mouse. *Microbiol. Immunol.* **39**: 555–562. [Medline] [CrossRef]
38. Umesaki, Y., Setoyama, H., Matsumoto, S., Imaoka, A. and Itoh, K. 1999. Differential roles of segmented filamentous bacteria and clostridia in development of the intestinal immune system. *Infect. Immun.* **67**: 3504–3511. [Medline]
39. Umesaki, Y., Setoyama, H., Matsumoto, S. and Okada, Y. 1993. Expansion of α β T-cell receptor-bearing intestinal intraepithelial lymphocytes after microbial colonization in germ-free mice and its independence from thymus. *Immunology* **79**: 32–37. [Medline]
40. van der Waaij, L. A., Limburg, P. C., Mesander, G. and van der Waaij, D. 1996. In vivo IgA coating of anaerobic bacteria in human faeces. *Gut* **38**: 348–354. [Medline] [CrossRef]
41. van Rees, E. P., Dijkstra, C. D., van der Ende, M. B., Janse, E. M. and Sminia, T. 1988. The ontogenetic development of macrophage subpopulations and Ia-positive non-lymphoid cells in gut-associated lymphoid tissue of the rat. *Immunology* **63**: 79–85. [Medline]
42. Varol, C., Vallon-Eberhard, A., Elinav, E., Aychek, T., Shapira, Y., Luche, H., Fehling, H. J., Hardt, W. D., Shakhar, G. and Jung, S. 2009. Intestinal lamina propria dendritic cell subsets have different origin and functions. *Immunity* **31**: 502–512. [Medline] [CrossRef]
43. Velaga, S., Herbrand, H., Friedrichsen, M., Jiong, T., Dorsch, M., Hoffmann, M. W., Förster, R. and Pabst, O. 2009. Chemokine receptor CXCR5 supports solitary intestinal lymphoid tissue formation, B cell homing, and induction of intestinal IgA responses. *J. Immunol.* **182**: 2610–2619. [Medline] [CrossRef]
44. Williams, R. C. and Gibbons, R. J. 1972. Inhibition of bacterial adherence by secretory immunoglobulin A: a mechanism of antigen disposal. *Science* **177**: 697–699. [Medline] [CrossRef]
45. Yamamoto, K., Qi, W. M., Yokoo, Y., Miyata, H., Udayanga, K. G. S., Kawano, J., Yokoyama, T., Hoshi, N. and Kitagawa, H. 2009. Histoplanimetrical study on the spatial relationship of distribution of indigenous bacteria with mucosal lymphatic follicles in alimentary tract of rat. *J. Vet. Med. Sci.* **71**: 621–630. [Medline] [CrossRef]
46. Yokoo, Y., Miyata, H., Udayanga, K. G. S., Qi, W. M., Takahara, E., Mantani, Y., Yokoyama, T., Kawano, J., Hoshi, N. and Kitagawa, H. 2011. Immunohistochemical and histoplanimetrical study on the spatial relationship between the settlement of indigenous bacteria and the secretion of bactericidal peptides in rat alimentary tract. *J. Vet. Med. Sci.* **73**: 1043–1050. [Medline] [CrossRef]
47. Yuasa, H., Mantani, Y., Masuda, N., Nishida, M., Arai, M., Yokoyama, T., Tsuruta, H., Kawano, J., Hoshi, N. and Kitagawa, H. 2017*a*. Mechanism of M-cell differentiation accelerated by proliferation of indigenous bacteria in rat Peyer's patches. *J. Vet. Med. Sci.* **79**: 1826–1835. [Medline] [CrossRef]
48. Yuasa, H., Mantani, Y., Masuda, N., Nishida, M., Kawano, J., Yokoyama, T., Hoshi, N. and Kitagawa, H. 2017*b*. Differential expression of Toll-like receptor-2, -4 and -9 in follicle-associated epithelium from epithelia of both follicle-associated intestinal villi and ordinary intestinal villi in rat Peyer's patches. *J. Vet. Med. Sci.* **78**: 1797–1804. [Medline] [CrossRef]